journal

J. Am. Ceram. Soc., 87 [10] 1864–1871 (2004)

Ultrasonic Spray Pyrolysis for Synthesis of Spherical Zirconia Particles

Y. L. Song,[†,‡] S. C. Tsai,[†,§] C. Y. Chen,[†] T. K. Tseng,[†] C. S. Tsai,[†,¶] J. W. Chen,[‡] and Y. D. Yao[††]

Institute for Applied Science and Engineering Research, Academia Sinica, Taipei, 115 Taiwan

Department of Chemical Engineering, California State University, Long Beach, California 90840

Department of Electrical Engineering and Computer Science, University of California, Irvine, California 92697

Department of Physics, National Taiwan University, Taipei, 106 Taiwan

Insititute of Physics, Academia Sinica, Taipei, 115 Taiwan

This paper presents new findings on ultrasonic spray pyrolysis of zirconium hydroxyl acetate precursor drops whose sizes were precisely measured using laser light diffraction technique. Precursor concentration plays a predominant role in determination of product particle size. At 0.01 wt% precursor concentration, conventional spray pyrolysis at 750°C using precursor drops 5–8 μm in diameter, generated by an ultrasonic nebulizer at 2.66 MHz, yielded *uniform* spherical yttria-stabilized zirconia (YSZ) particles 73 nm in diameter measured by scanning electron microscopy. The YSZ particle diameters were much smaller than those predicted by the one-particle-per-drop mechanism. Under similar reaction conditions, the high-throughput ultrasound-modulated two-fluid (UMTF) spray pyrolysis of larger precursor drops (28-μm peak diameter) also yielded spherical dense particles; they were significantly *smaller* in size than those produced by the low-throughput conventional ultrasonic spray pyrolysis of smaller drops (6.8-μm peak diameter).

I. Introduction

SPRAY PYROLYSIS is widely used in industry to produce fine-grained powders (>0.5-μm diameter) because it is an inexpensive continuous process that requires only ambient pressure conditions. In addition, spray pyrolysis allows synthesis of a variety of advanced ceramic powders and films because it can be used with various chemicals.[1] To generate precursor drops in spray pyrolysis, two commonly used atomization techniques are two-fluid atomization[2,3] (liquid atomization by high-velocity air) and ultrasonic atomization[3–5] (without air). The two techniques vary in terms of their throughput and the size distribution of the drops they produce. While two-fluid atomization has the advantage of high throughput, it has the disadvantage of broad drop-size distribution. In contrast, while ultrasonic atomization has the advantage of narrow drop-size distribution, it has the disadvantage of low throughput.[3] The micrometer-sized particles (>0.5-μm diameter) produced in spray pyrolysis using these two atomization techniques are often broken and irregular in shape.[4]

A third technique, called ultrasound-modulated two-fluid (UMTF) atomization,[6–8] for generating precursor drops in spray pyrolysis capitalizes on the advantages of the two atomization techniques described above. Specifically, it has the advantages of high throughput, narrow drop-size distribution, and much smaller peak drop diameter (the diameter where the peak of a drop-size distribution occurs) than that of conventional ultrasonic atomization at the same ultrasonic frequency. Air-assisted ultrasonic (or UMTF) spray pyrolysis uses UMTF atomization to generate drops; the drops flow through a tubular reactor under pyrolysis conditions and are converted into oxide particles.

In this paper, data presented demonstrate that UMTF spray pyrolysis is capable of producing significantly smaller particles than conventional ultrasonic spray pyrolysis, and at a significantly lower ultrasonic frequency. Specifically, we compared the sizes and size distributions of particles produced by spray pyrolysis of precursor drops of very different sizes and size distributions generated by UMTF atomization at 120 kHz and conventional ultrasonic nebulizer atomization at 1.65 MHz. We found that despite much larger precursor drop sizes (peak diameter, 28 μm in UTMF atomization versus 6.8 μm in atomization via conventional methods), UMTF spray pyrolysis at 120-kHz ultrasonic frequency and 2.3-W electric drive power generated a higher percentage (70% with UMTF versus 11% with the conventional nebulizer) of yttria-stabilized zirconia (YSZ) particles that were smaller than 0.35-μm diameter. In addition, this paper reports the influences of reaction temperature and precursor solution concentration on particle size and morphology in spray pyrolysis. Since precursor drops with precisely measured sizes and very narrow drop-size distributions were used, it was possible to compare the particle diameters produced to the predicted values based on the one-particle-per-drop mechanism. The results show that precursor vaporization took place to a very significant degree and the gas-to-particle conversion mechanism was also active.

II. Experimental Procedure

(1) Precursor Solution Preparation and Precursor Drop Size Analysis

The precursor used in this study was zirconium hydroxyl acetate (ZHA) containing yttrium acetate hydrate (YAH) in the molar ratio of 3:97 Y_2O_3/ZrO_2. Both salts were reagent grade (99+% purity) from Aldrich Chemical (Milwaukee, WI). The chemical formula of ZHA was $Zr(OH)_x(CH_3COO)_{4-x}$, where $x = 2.64$, and the molecular weight was 216 with the weight fraction of ZrO_2 being 0.57. The chemical formula of YAH is $(CH_3COO)_3Y$ with a molecular weight of 266 and 10 wt% hydrated water. Since only a very small amount of YAH was used in precursor solutions, the hydrated water in YAH was neglected in the calculation of

R. Cutler—contributing editor

Manuscript No. 10067. Received April 1, 2003; approved May 19, 2004.

This work was financially supported by the National Science Foundation (USA) under Grant No. CTS-98120050 and the National Science Council under Grant Nos. NSC-89-2216-E-01-005, NSC-90-2216-E-001-001, and NSC-89-2811-E-036-0004, and the Academia Sinica, Taiwan.

[†]Institute of Applied Science, Academia Sinica.
[‡]National Taiwan University.
[§]California State University.
[¶]University of California, Irvine.
[††]Institute of Physics, Academia Sinica.

precursor concentrations. The precursor was characterized by thermal gravitational analysis (TGA) and differential scanning calorimetry (DSC) analysis. TGA was conducted in a Perkin-Elmer Model TGA-7 under nitrogen flow for removal of product gases. DSC was conducted in a closed system (Dupont Model 2010). The difference between the sample and reference cells in the heat required to reach a given temperature at a specified heating rate was recorded as a function of temperature.

Precursor solutions at a concentration ranging from 0.01 to 5.0 wt% were prepared by dissolving yttrium-containing ZHA in deionized water. A precursor concentration of 5.0 wt% was used unless specified otherwise. The surface tension and the kinematic viscosity of the precursor solution were measured using a Kruss Digital Tensiometer K9 and a Cannon-Fenske viscometer, respectively. They were found to resemble those of deionized water.

Drop sizes and drop-size distributions were measured using a Malvern Spraytec RTS 5000. This instrument uses a solid-state laser light to illuminate the drops. The scattered lights are collected from the forward direction by a log-scaled Fourier transform lens and analyzed using Fraunhoffer diffraction theory.[9] The refractive index of water (1.33) is used in the analysis because of the low precursor concentration. The resulting drop-size and size distributions are presented as frequency plots of volume percentage versus drop diameter using a semilogarithmic scale. The instrument, limited to particles larger than 0.5-μm diameter, was calibrated using a reticle, Malvern/INSITEC Model No. RS-3.

(2) Spray Pyrolysis System

Figure 1 provides a schematic diagram of the spray pyrolysis system used in this study. Major components of the system are as follow: (1) a three-zone furnace 130 cm in length (Linberg Model Blue M) capable of heating to a maximum temperature of 1100°C, (2) a 7.6- or 2.5-cm i.d. tubular quartz reactor (170-cm length) located in the furnace, (3) an atomizer/nebulizer with a power supply system for generation of precursor drops, and (4) precision flow meters and controllers (MKS Model 1179, Andover, MA). As shown in this figure, carrier air is supplied upstream and a vacuum pump is provided downstream from the reactor for control of the residence time of the precursor drops flowing through the reactor. The resulting product particles are collected in the cold traps and on the filter positioned between the traps and the vacuum pump.

The 7.6-cm tubular reactor was used unless specified otherwise. As shown in Fig. 2, the temperature of zone 2 of the furnace was set at the maximum reaction temperature (650°, 700°, and 750°C), while the temperatures of zone 1 and zone 3 were set at 200° and 350°C, respectively. The liquid flow rate was maintained at 5 cm^3/min for the UMTF atomizer but less than 0.3 cm^3/min for the nebulizers. The rates of airflow through the reactor ranged from 20 to 31 L/min at standard conditions. The temperatures, at several points along the axis of the 7.6-cm tubular reactor, were measured using a type K (NiCr-NiAl) thermocouple with an accuracy of ±2.5°C. These temperatures, independent of the air and liquid flow rates, are shown in Fig. 2. On the basis of the temperature profiles in this figure, the flow rates of carrier air along the axis of the reactor were first calculated for three different flow rates (20, 25, and 31 L/min at standard conditions) assuming ideal gas. Division of the flow rates by the cross-sectional area of the tubular reactor gave rise to the carrier air velocities along the reactor axis, yielding the temperature–residence time profiles for air-entrained drops or particles near the axis in both 7.6- and 2.5-cm tubular reactors. From these profiles, the residence time at the same maximum reactor temperature and carrier airflow rate was found to decrease by 1 order of magnitude as the tube diameter was reduced from 7.6 to 2.5 cm. For example, at a maximum reactor temperature of 650°C and a carrier airflow rate of 31 L/min at standard conditions, the residence time at temperatures of 550°C and above was reduced from 2.2 s to an estimated value of 0.2 s.

The UMTF atomizer used in this study consists of an annulus for airflow and an ultrasonic nozzle (Sono-Tek Model 8700-120, Milton, NY) with a central channel (0.93 ± 0.02-mm diameter) for liquid flow.[7] The Sono-Tek ultrasonic nozzle is a half-wavelength design with a resonant frequency of 120 kHz. It is geometrically configured such that excitation of the piezoelectric transducers creates a standing wave through the nozzle, with the maximum

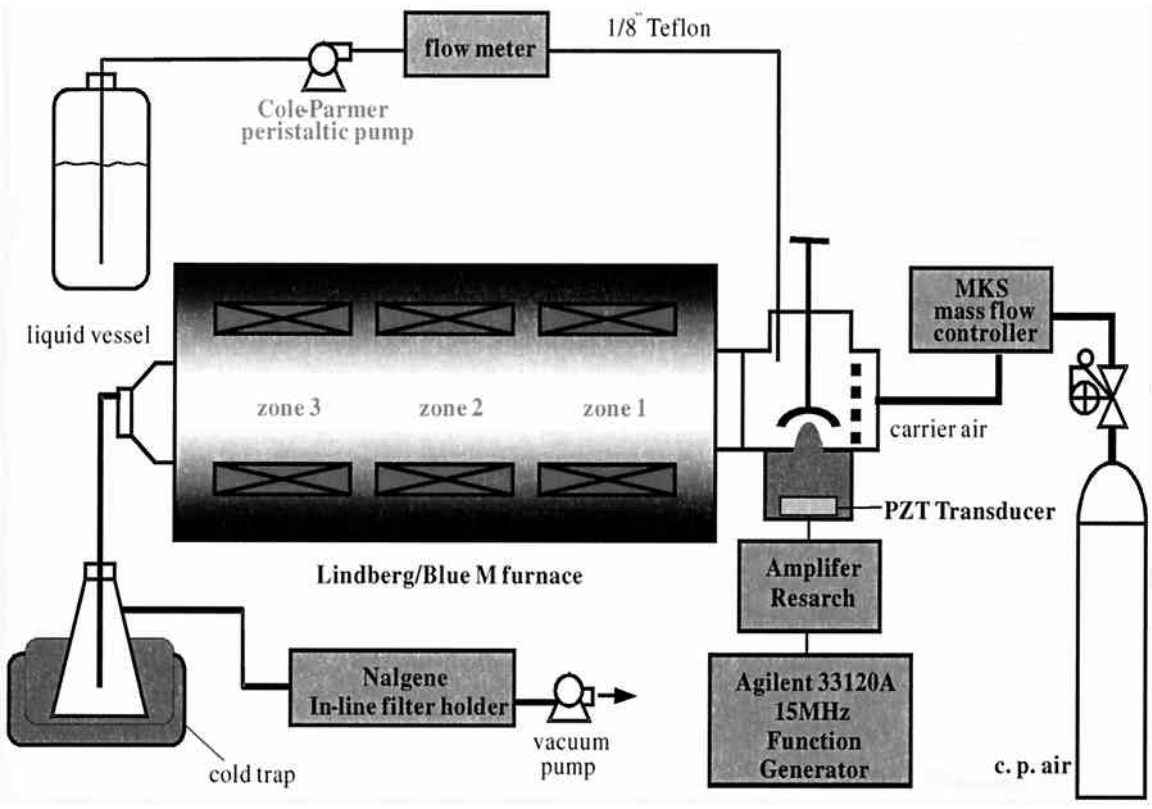

Fig. 1. Schematic diagram of spray pyrolysis system.

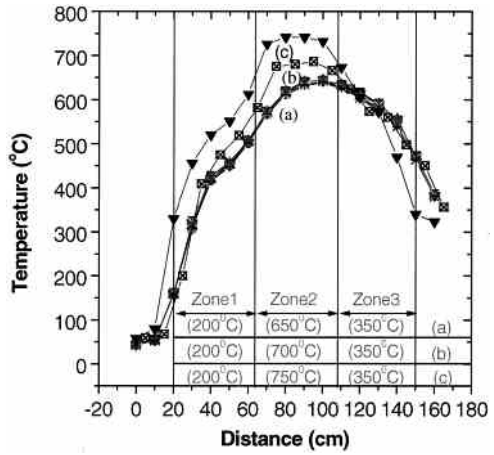

Fig. 2. Temperature profile of the three–zone 7.6-cm-diameter tubular reactor of the spray pyrolysis system at maximum reactor temperatures of (a) 650°, (b) 700°, and (c) 750°C (measurement error ±2.5°C).

vibration amplitude occurring at the nozzle tip. As a liquid jet issues from the nozzle tip, a liquid capillary wave is generated with amplitude growing exponentially due to amplification by the air blowing around it.[8] Atomization (or spray) occurs when the amplitude becomes too great to maintain wave stability, yielding precursor drops with 28-μm peak diameter.

Ultrasonic nebulizers (or disk transducers) with resonant frequencies of 1.65 and 2.66 MHz (King Ultrasonics Co., Ltd., Taipei, Taiwan) were also used in this study to generate uniform drops smaller than 10-μm diameter. Unlike the Sono-Tek ultrasonic nozzle, the precursor solution was in direct contact with the PZT transducer disk in the nebulizer, as shown in Fig. 1. The cap above the transducer was adjusted so that only the precursor drops with a narrow size range (6–9- and 5–8-μm diameter for 1.65- and 2.66-MHz nebulizers, respectively) passed through the tubular reactor. The drop sizes produced by the nebulizers were much smaller than those produced by the UMTF atomizer, but the throughput was 1 order of magnitude smaller, and the electric drive power required for atomization was almost 1 order of magnitude larger. Furthermore, spray performance of the nebulizer deteriorated due to its transducer being in direct contact with the precursor solution. The experimental conditions for spray pyrolysis using a nebulizer were rather limited as a result.

(3) Product Particle Characterization

The product particles were characterized by X-ray diffraction (XRD) using Model MXP-18, MacScience Co., Japan. The size and morphology of the product particles were determined using field emission scanning electron microscopy (SEM, Hitachi Model S-4200, Japan). A set of 10–20 SEM micrographs was obtained for each spray pyrolysis experiment from which two to four representative graphs were selected for counting of particles to determine the particle-size distribution and mean particle diameter. The total number of particles counted to obtain a particle-size distribution ranged from 800 to as many as 1350. The accuracy of the (number) mean diameter was found to be ±4% or better.

III. Results and Discussion

As the precursor drops flow through the spray pyrolysis reactor, they undergo three major steps: (1) drop evaporation, (2) conversion of precursor into oxides, and (3) particle formation. The effects of the reaction temperature, the precursor solution concentration, and the precursor drop size on product particle sizes and size distributions are discussed in this section after a description of the precursor pyrolysis properties and the sizes and size distribution of the precursor drops.

(1) Chemical Characterizations of Precursor and Product Particles

The TGA curves in Fig. 3(a) show a slightly lower residual weight fraction (0.55 vs 0.57) as a result of ~4% water adsorption on the samples used. In Fig. 3(b), the second run uses the same sample as the first run, but without the volatiles that have been removed in the first run. Figure 3(a) shows 10% water loss and, thus, indicates that the $Zr(OH)_x$ group in the ZHA used may exist partially as zirconyl oxide hydrate $ZrO{\cdot}H_2O$. Using 96% as a weight correction factor, complete conversion of ZHA to $Zr(OH)_4$ should yield a residual weight of 71%, as indicated in the figure.

On the basis of Fig. 3(a), four different weight loss mechanisms take place in temperature ranges of 50°–150°, 150°–300°, 300°–400°, and 400°–600°C. The weight loss in temperature ranges 50°–150° and 400°–600°C can be attributed to water evaporation and conversion into ZrO_2. Weight loss in the two middle temperature ranges may be attributed to decomposition of ZHA to acetic acid and $Zr(OH)_4$ and subsequent evaporation of the products. This interpretation is born out by the DSC curves in Fig. 3(b). This

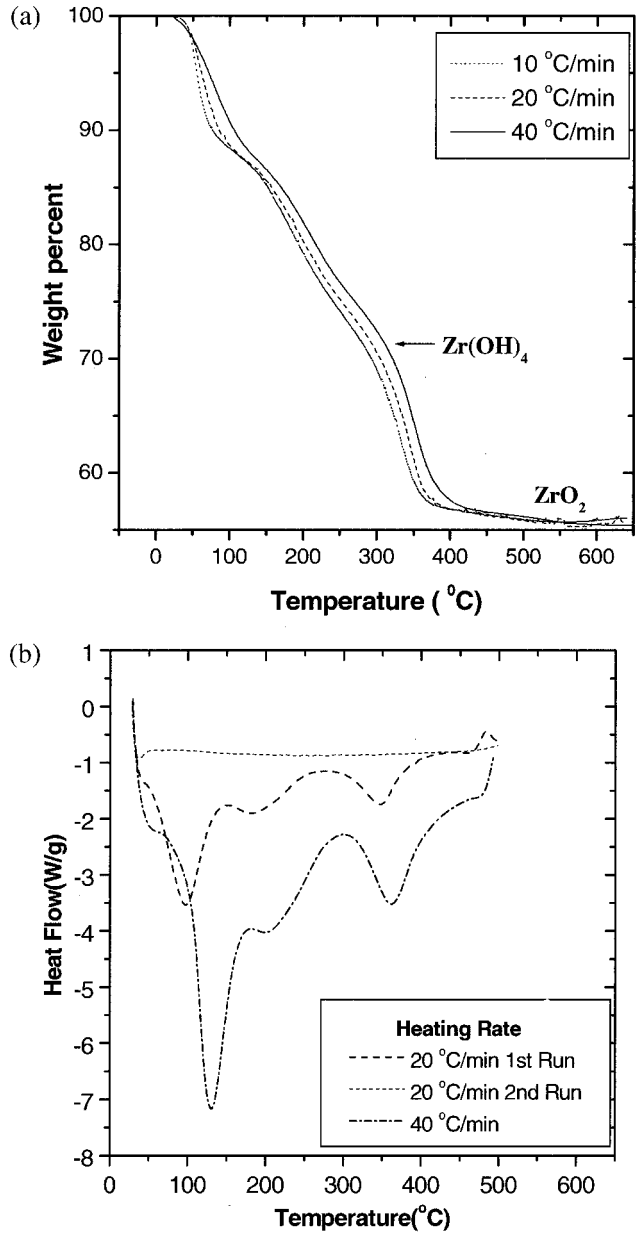

Fig. 3. (a) Thermal gravitational analysis (TGA) and (b) differential scanning calorimetric (DSC) analysis of precursor zirconium hydroxyl acetate (ZHA).

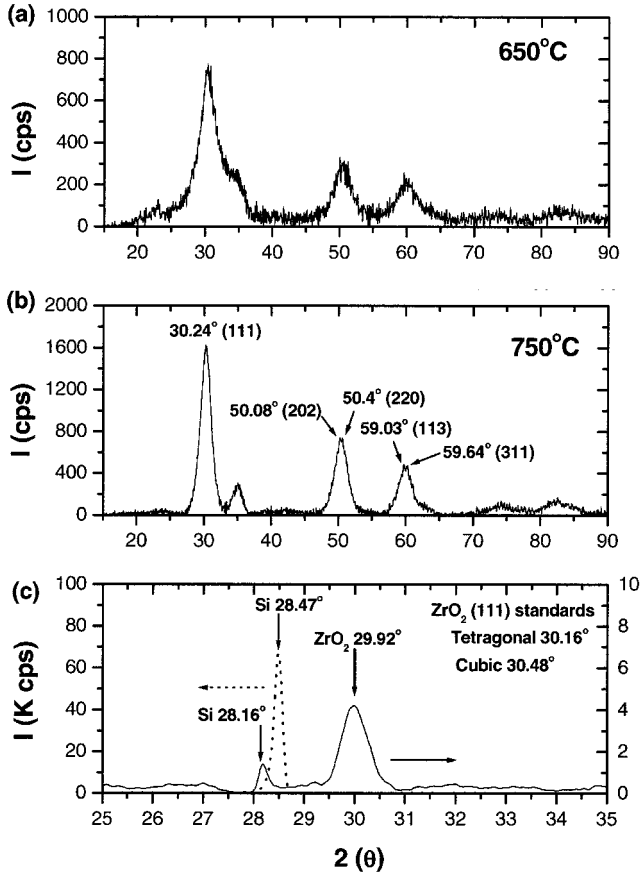

Fig. 4. XRD patterns for product particles as-received from spray pyrolysis at (a) 650° and (b) 750°C, and (c) dotted curve for pure silicon (reference) and solid curve for a mixture of silicon and product particles in (a) annealed at 800°C for 30 min.

figure shows the heat absorption reaction at 100°C due to water evaporation and the exothermic reaction near 500°C due to conversion into ZrO_2. It also shows two heat absorption peaks at 175° and 350°C. The 175°C peak may be attributed to evaporation of acetic acid (normal boiling point in pure state, 120°C). Formation of acetic acid was confirmed by an acidity test (pH ~ 2) of the liquid product collected in pyrolysis of ZHA at 325°C. The 350°C peak may be attributed to evaporation of zirconium hydroxide (amorphous white powder).

The XRD patterns of the particles as-received from spray pyrolysis at reaction temperatures of 650° and 750°C are shown in Figs. 4(a) and (b), respectively. The XRD signals in Fig. 4(a) are less sharp. However, after annealing these particles at 800°C for 30 min, the XRD signals were found to be identical to those in Fig. 4(b). The sharp XRD signals in Fig. 4(b) were identified as YSZ, tetragonal phase,[10] on the basis of the splits of XRD signals around 50° and 59°. Specifically, the split 50.8° and 50.4° results from tetragonal (202) and (220) planes, and the split 59.03° and 59.64° results from tetragonal (113) and (311) planes. In addition, Fig. 4(c) shows the XRD signals for the annealed particles mixed with silicon as a reference. The 29.92° peak in Fig. 4(c), red-shifted by 0.31° (difference in silicon lines 28.47°–28.16°), corresponds to the 30.24° peak in Fig. 4(b), which is closer to ZrO_2 (111) standards for tetragonal than for cubic (30.16° vs 30.48°). Therefore, the crystal phase of the YSZ particles is tetragonal rather than cubic in good agreement with the reported tetragonal phase for 3YSZ zirconia[10] and for the nanoparticles obtained in combustion spray pyrolysis.[11]

(2) Drop Size and Size Distribution

The drop sizes and size distributions of the atomized precursor solutions used in this study are given in Fig. 5. In this figure, MMD

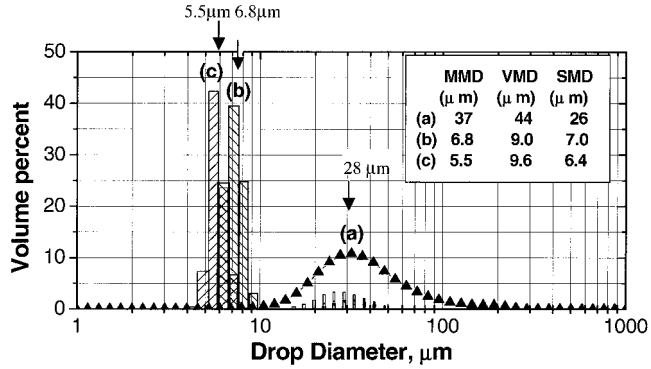

Fig. 5. Drop-size distributions for (a) ultrasound-modulated two-fluid (UMTF) atomization at 120 kHz, 2.3 W, 150 m/s air velocity, and 4.1 mA/mL, (b) ultrasonic atomization using a modified industrial nebulizer at 1.65 MHz and 23.5 W, and (c) ultrasonic atomization using a homemade nebulizer at 2.66 MHz and 20 W.

(mass median diameter) designates the drop diameter at 50% of the cumulative drop-size distribution; VMD (volume mean diameter) and SMD (Sauter mean diameter) are the mean diameters of the drops based on the volume and surface, respectively. Curve (a) represents the drop size distribution by UMTF atomization (at ultrasonic frequency of 120 kHz, electric drive power of 2.3 W, and atomization air velocity of 150 m/s). The drop diameters range from 10 to 90 μm. The peak diameter, MMD, and VMD are 28 μm, 37 μm, and 44 μm, respectively.

As shown in Fig. 5, histograms (b) and (c), the drops generated in this study by the nebulizers with the PZT disk transducers at respective resonance frequencies of 1.65 and 2.66 MHz and respective electric drive power levels of 24 and 20 W are uniform in size with the exception of a small amount of drops of 20–50-μm diameter. Specifically, the drop sizes range from 6 to 9 μm with peak diameter of 6.8 μm for the 1.65-MHz nebulizer and from 5 to 8 μm with peak diameter of 5.5 μm for the 2.66-MHz nebulizer. The respective VMDs are 9 and 9.6 μm due to the presence of small amounts of 20–50-μm drops. The calculated drop diameters at ultrasonic frequencies of 1.65 and 2.66 MHz are 8.7 and 6.4 μm based on the Kelvin equation for capillary wavelength with a proportionality constant of unity[6,7] (experimentally determined for a correlation between peak drop diameters and capillary wavelengths for ultrasonic frequency ranging from 54 to 360 kHz). Excluding the small amounts of 20–50-μm drops, these precursor drops are rather uniform in size. Therefore, the peak drop diameter is used in calculation of the (number) mean particle diameter based on the one-particle-per-drop mechanism to be presented in Results and Discussion. It should be pointed out that a proportionality of 0.34 was first presented by Lang[12] and subsequently used in many spray pyrolysis studies[3,5] for calculation of precursor drop diameters, resulting in considerably underestimated values. It should also be noted that the small amounts of drops 20–50-μm diameter generated by the nebulizers may account for the presence of a few large particles seen in the SEM micrographs of the resulting particles to be presented later.

(3) Effects of Reaction Temperature

The effects of pyrolysis temperature on the YSZ particle size and morphology were investigated using the 6–9-mu]m precursor drops generated by the 1.65-MHz nebulizer. The spray pyrolysis was conducted in a 7.6-cm-diameter reactor at two reaction temperatures (700° and 650°C), a constant precursor concentration of 1.0 wt%, and a carrier airflow rate of 20 L/min at standard conditions. The resulting YSZ particle-size distributions are shown in Figs. 6(a) and (b) for 650° and 700°C, respectively. This figure shows that the sizes and size distributions of the spherical particles produced at 650° and 700°C are quite similar. No significant effect of pyrolysis temperature on particle size and size distribution was seen in the spray pyrolysis of the 6–9-μm drops at 0.2 wt%

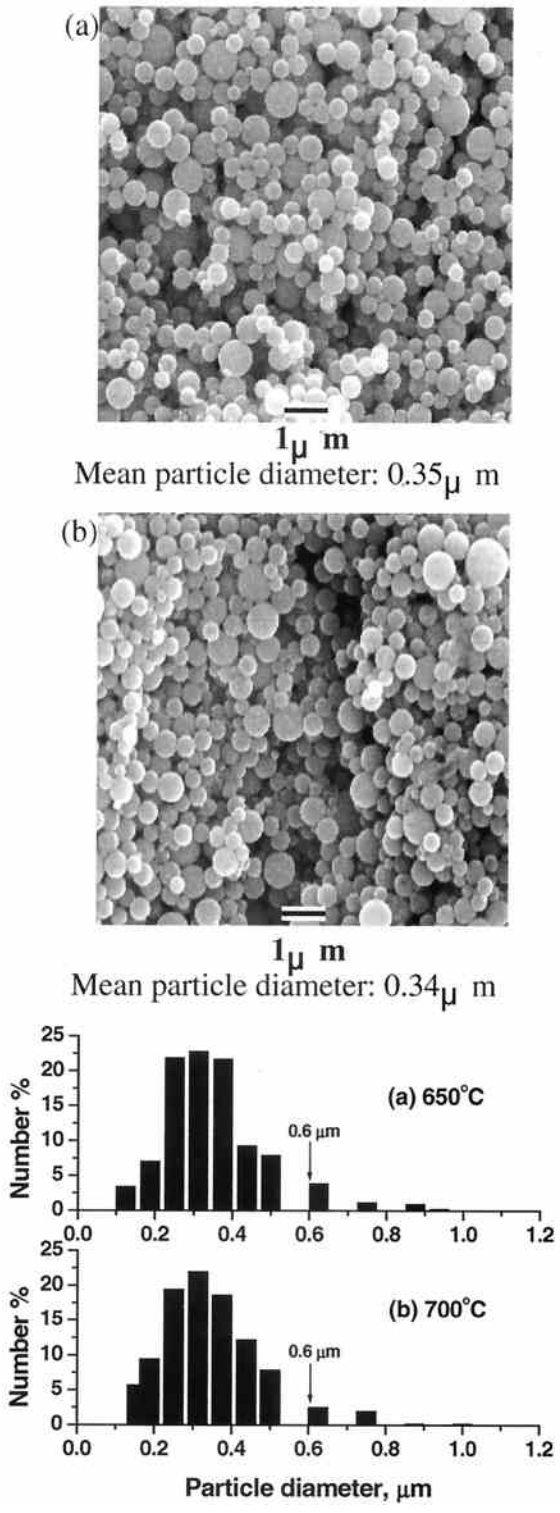

Fig. 6. SEM micrographs and particle size distributions for spray pyrolysis of the 6–9-μm precursor drops at 1.0 wt% precursor solution, 20 L/min (at standard conditions) carrier airflow rate, and maximum reactor temperature of (a) 650° and (b) 700°C using a 7.6-cm-diameter tubular reactor.

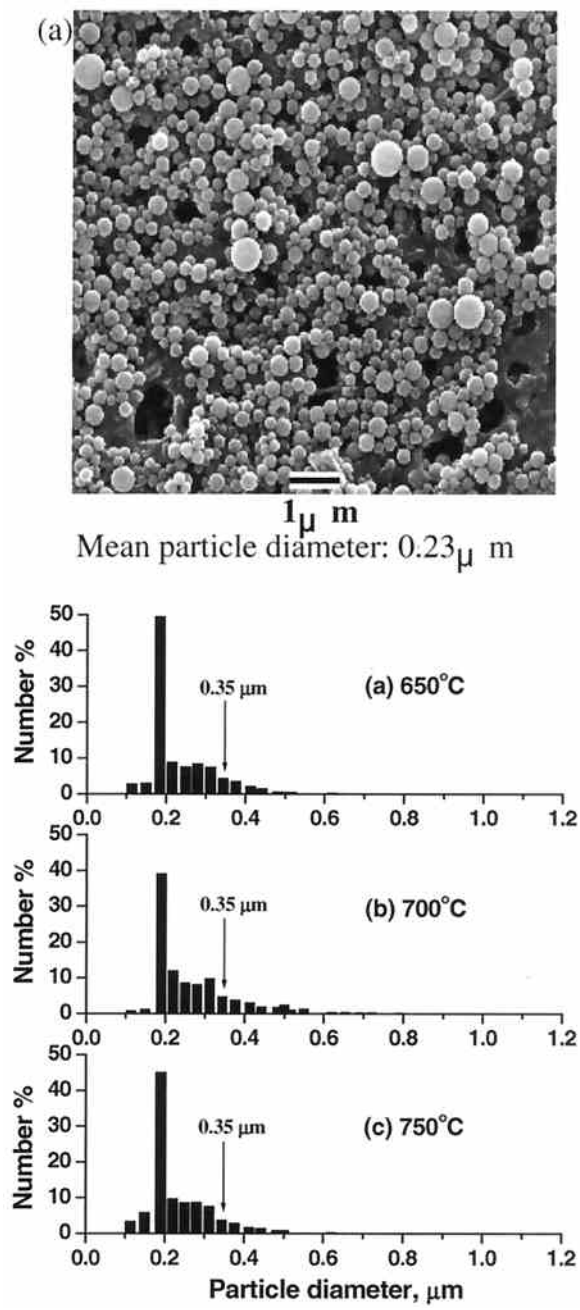

Fig. 7. SEM micrograph and particle size distributions for spray pyrolysis of the 6–9-μm precursor drops at 0.2 wt% precursor solution, 20 L/min (at standard conditions) carrier airflow rate, and maximum reactor temperature of (a) 650°, (b) 700°, and (c) 750°C using a 7.6-cm-diameter tubular reactor.

precursor concentration either, even when the temperature was increased to 750°C (carrier airflow rate still at 20 L/min at standard conditions). Specifically, Figs. 7(a)–(c) show that the particle size distributions obtained at 650°, 700°, and 750°C are similar with a mean diameter of 0.23 ± 0.02 μm. It should be noted that, for the 7.6-cm reactor, an increase in the maximum reactor temperature from 650° to 750°C resulted in an increase in residence time at temperatures of 550°C and above from 3.2 to 4.5 s.

Thus, increases in temperature ranging from 650° to 750°C affect spray pyrolysis product particles by sharpening the XRD patterns. The effect of temperature on particle size and morphology is negligible in the studied narrow drop size range (6–9 μm) and long residence time (3.2–4.5 s).

(4) Effects of Precursor Concentration

To examine the effect of precursor concentration on the product particle size and morphology, the 6–9-μm drops at 5.0 wt% precursor concentration were also subjected to spray pyrolysis at 650°C and a carrier airflow rate of 20 L/min at standard condtions. The resulting SEM micrograph and particle size distribution are shown in Fig. 8. Comparisons of Fig. 8 to Fig. 6(a) and Fig. 7(a)

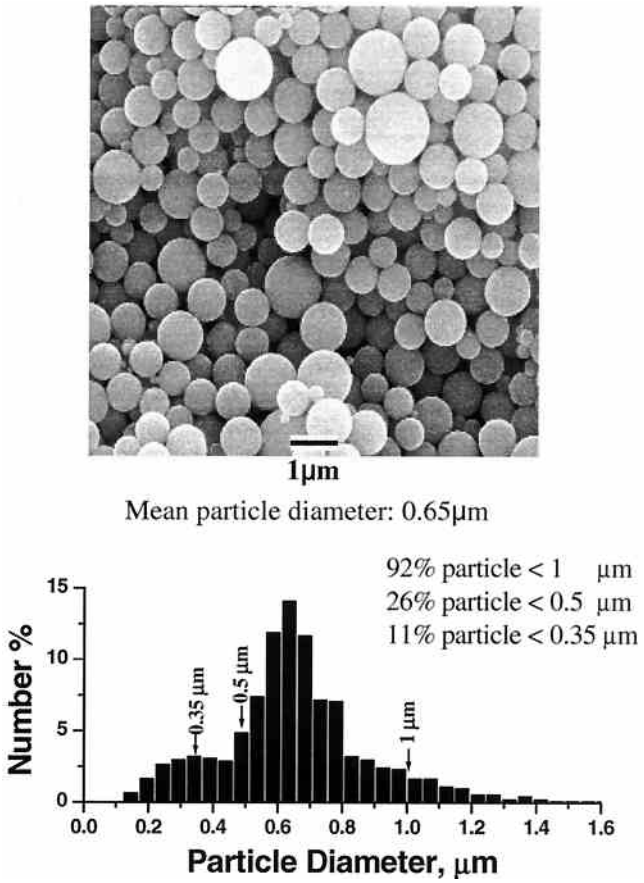

Fig. 8. SEM micrograph and particles size distribution of the YSZ particles obtained from spray pyrolysis of the 6–9-μm drops at 5.0 wt% precursor solution, 20 L/min (at standard conditions) carrier airflow rate, and maximum reactor temperature of 650°C using a 7.6-cm-diameter tubular reactor.

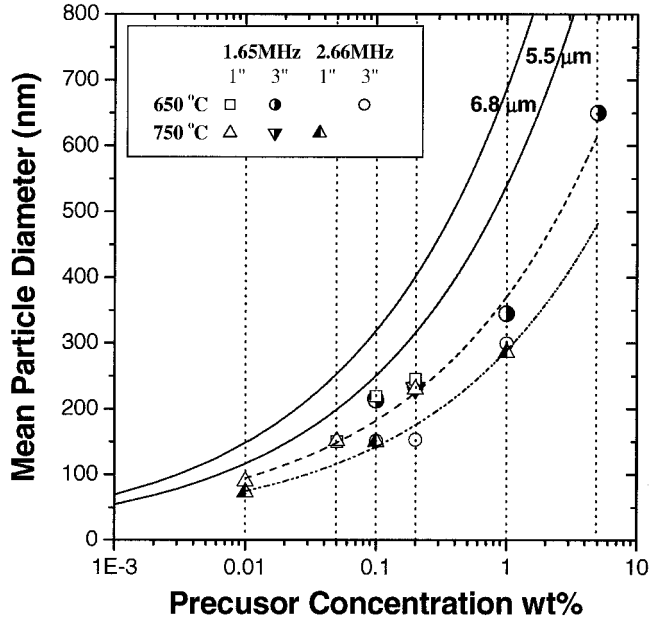

Fig. 9. Effects of precursor concentration on mean particle diameter (where "1E−3" represents 1×10^{-3}). Data points along the best-fit dotted curves are mean particle diameters obtained from SEM micrographs. Two solid curves are theoretical mean particle diameters based on the one-particle-per-drop mechanism for peak precursor drop diameters of 6.8 and 5.5 μm generated at ultrasonic frequencies of 1.65 and 2.66 MHz, respectively.

clearly show the drastic effect of decreasing precursor concentration. As the precursor concentration decreases, the particle sizes decrease, and the size distribution becomes narrower. The (number) mean particle diameters are 0.65, 0.35, and 0.23 μm for precursor concentrations of 5.0, 1.0, and 0.2 wt%, respectively. The corresponding size ranges are 0.17–1.42, 0.13–0.94, and 0.13–0.45 μm. Similar effects are seen at 700°C pyrolysis temperature as shown by comparing Fig. 6(b) to Fig. 7(b).

Figure 9, in semilogarithmic scale, depicts the effect of precursor concentration on (number) mean particle diameter in spray pyrolysis at temperatures of 650° and 750°C of precursor drops of 6–9- and 5–8-μm diameter (with respective peak diameters of 6.8 and 5.5 μm) generated by the 1.65- and 2.66-MHz nebulizers, respectively. In this figure, the data points along the best-fit dotted curves were obtained from the SEM micrographs; the solid curves were predicted by the one-particle-per-drop mechanism (Eq. (1) to be presented later) for precursor drop diameters of 6.8 and 5.5 μm. Both the experimental data and the theoretical curves show decreased mean particle diameter with decreasing precursor concentration. However, the experimental values were considerably smaller than the theoretical values predicted for the corresponding peak drop diameters. For example, the measured mean particle diameter decreased from 650 to 350 nm as the precursor concentration decreased from 5.0 to 1.0 wt% for precursor drops with 6.8-μm peak diameter. The mean particle diameter decreased further to 73 nm with further decrease in precursor concentration to 0.01 wt% and a slight decrease in precursor drop size from 6.8- to 5.5-μm peak diameter. It is interesting to note that grain sizes of 74–265 nm were reported[13] in the columnar structure of a YSZ thin film (0.1-μm thickness) grown by ultrasonic spray pyrolysis at ambient pressure and a substrate temperature ranging from 600° to 750°C using a 1.7-MHz ultrasonic nebulizer for a precursor solution (zirconium octylate dissolved in a mixed solvent of toluene and 2,4-pentanedione) with 2 wt% metallic (equivalent to 4.75 wt% ZHA).

(5) Comparison of UMTF to Conventional Ultrasonic Nebulizer Spray Pyrolysis

The one-particle-per-drop mechanism of spray pyrolysis[1] predicts that particle size is positively correlated with precursor drop size (i.e., the larger the precursor drop, the larger the resulting particles). We examined whether such expected effects occurred by comparing the SEM micrograph and the particle size distribution in Fig. 8 for the 6–9-μm precursor drops of 6.8-μm peak diameter with those in Fig. 10 for UMTF atomized drops with 28-μm peak diameter. The spray pyrolysis conditions were 650°C maximum temperature and 5.0 wt% precursor concentration in both cases. The carrier airflow rate and liquid flow rate are 20 L/min at standard conditions and less than 0.3 cm^3/min for the 6–9-μm drops; the respective values are 31 L/min at standard conditions and 5 cm^3/min for the UMTF atomized drops with 28-μm peak diameter. As predicted by the one-particle-per-drop mechanism, the YSZ particles in Fig. 8 are more uniform in size than those in Fig. 10, due to the narrower precursor drop-size distribution in Fig. 5(b) than that in Fig. 5(a). However, while more than 80% of the YSZ particles in Fig. 10 are smaller than 0.5-μm diameter, only 26% of those in Fig. 8 are, despite the much larger sizes (28- vs 6.8-μm peak diameter) of the UMTF atomized precursor drops. The percentage of the YSZ particles smaller than 0.35 μm is also higher using the UTMF atomizer (70%, Fig. 10) than using the conventional ultrasonic nebulizer (11%, Fig. 8). Furthermore, as much as 97% of the particles in Fig. 10 and 92% in Fig. 8 are smaller than the 1.0-μm diameter expected for spray pyrolysis of precursor drops of 6-μm diameter at 5.0 wt% precursor concentration, based on the one-particle-per-drop mechanism (see Table I).

(6) Comparison to Predictions by the One-Particle-per-Drop Mechanism

In the one-particle-per-drop mechanism of spray pyrolysis,[1] each precursor drop serves as a microreactor whose temperature varies as it travels along the three-zone tubular reactor. As the water evaporates,

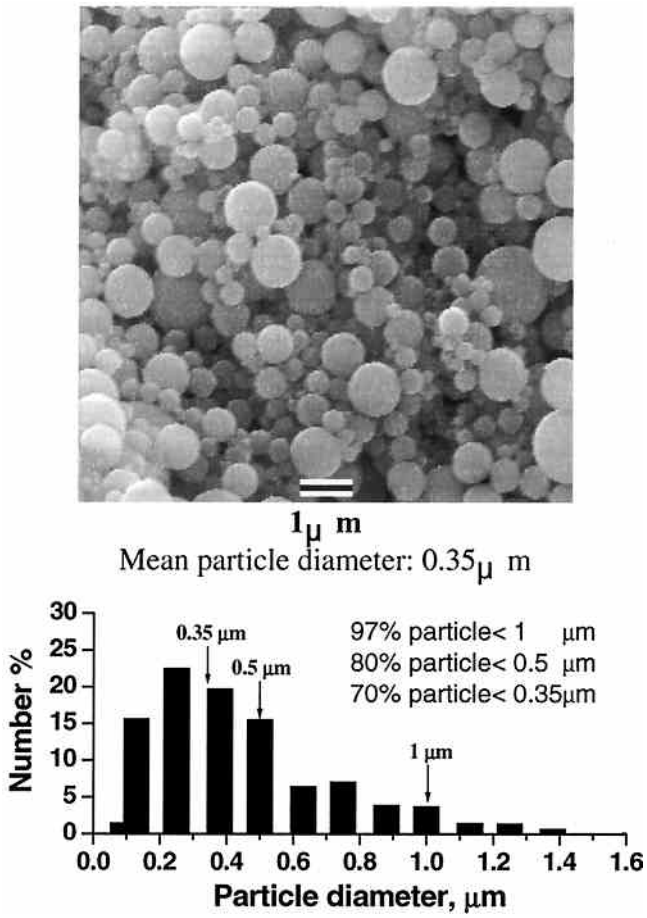

Fig. 10. SEM micrograph and particles size distribution of the YSZ particles obtained from UMTF spray pyrolysis at 5.0 wt% precursor solution, 31 L/min (at standard conditions) carrier airflow rate, and maximum reactor temperature of 650°C using a 7.6-cm-diameter tubular reactor.

the diameter of the precursor drop decreases, and the precursor concentration increases. Eventually, the precursor drop is completely dehydrated, and the precursor is converted into oxides with no phase change, resulting in a dense spherical solid particle. (The BET analysis indeed shows very low specific surface area.) Assuming no precursor is vaporized and conversion into oxides takes place within the drop, a mass balance based on conservation of ZrO_2 results in the following simple relationship between the particle diameter (d_p) and the precursor drop diameter (d):

$$d_p = d \sqrt[3]{\frac{\rho_s w}{\rho_p}} \quad (1)$$

where w is the precursor concentration in terms of weight fraction of ZrO_2; ρ_s and ρ_p are the densities of the precursor solution (1 g/cm^3) and zirconia ZrO_2 (6 g/cm^3), respectively.[10] Using this equation, particle diameters for the precursor drop diameters ranging from 6 to 9 μm and precursor concentrations of 0.01, 0.2, 1.0, and 5.0 wt% ZHA were calculated and are presented in Table I. Careful examinations of Figs. 7–9 reveal that less than 10% of the particles produced are of the sizes predicted by this simple model for the 6-μm-diameter drops. Figure 11(a) also shows that more than 90% of the product particles obtained by spray pyrolysis of 5–8-μm-diameter drops in a 2.5-cm-diameter reactor at a maximum reactor temperature of 750°C for 0.01 wt% precursor concentration are smaller than 120-nm

Table I. Theoretical Diameters of Dense Spherical Zirconia Particles (Based on the One-Particle-per-Drop Mechanism of Spray Pyrolysis)

Precursor drop diameter (μm)	Zirconium–hydroxyl–acetate (precursor) concentration			
	0.01 wt%	0.2 wt%	1.0 wt%	5.0 wt%
6	0.13	0.35	0.6	1.0
7	0.15	0.4	0.7	1.2
9	0.19	0.51	0.9	1.5

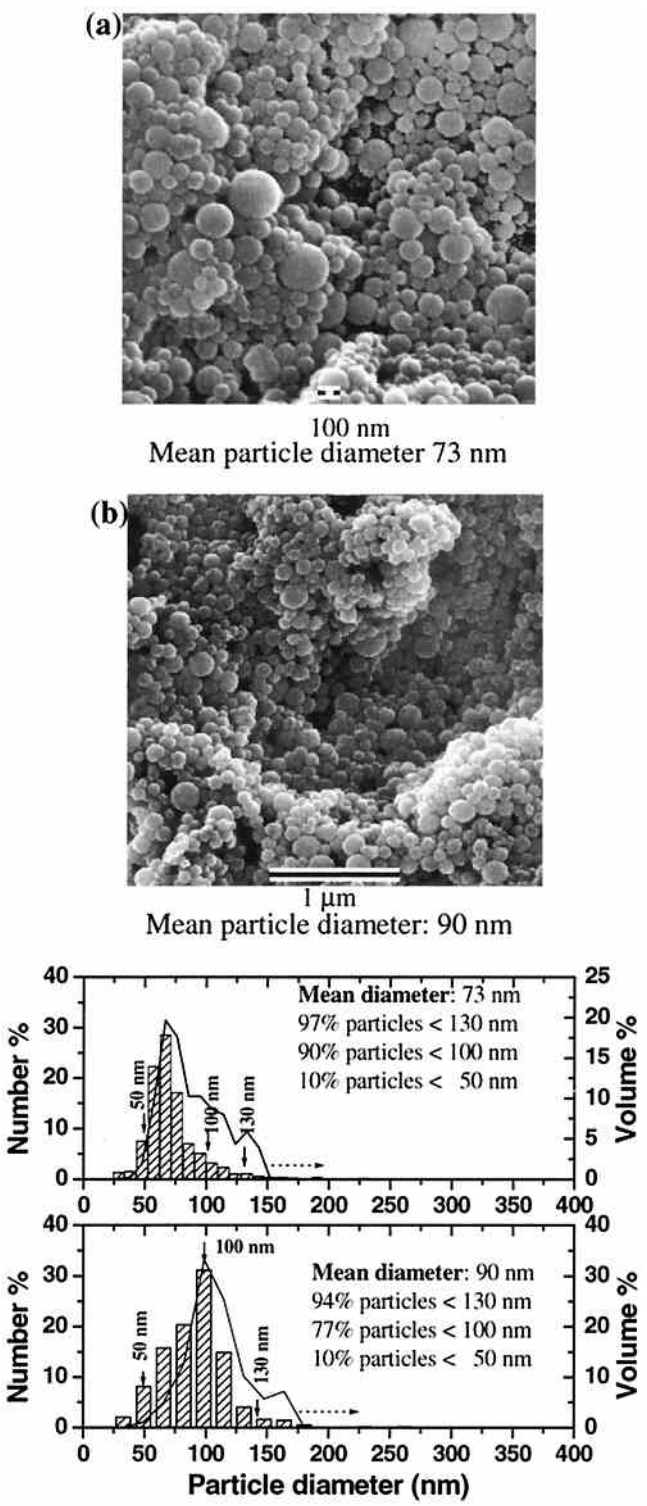

Fig. 11. SEM micrograph and particle size distribution of YSZ particles obtained from spray pyrolysis using a 2.5-cm-diameter tubular reactor at 0.01 wt% precursor solution, 31 L/min (at standard conditions) carrier airflow rate, maximum reactor temperature of 750°C, and precursor drop diameters of (a) 5–8 and (b) 6–9 μm.

diameter (predicted by the one-particle-per- drop mechanism for the precursor drops of 5.5-μm diameter, as shown in Fig. 9).

Furthermore, (number) mean particle diameters of 73 and 90 nm, as shown in Fig. 11, were obtained in spray pyrolysis of precursor drops (0.01 wt% precursor concentration) with peak drop diameters of 5.5 and 6.8 μm, which should have produced particle diameters of 120 and 150 nm on the basis of Eq. (1); the experimental mean particle diameters were only 60% of these predicted values. Likewise, examinations of Figs. 6–8 also reveal that the experimental mean particle diameters were 60%, 58%, and 65% of the theoretical values predicted by the one-particle-per-drop mechanism Eq. (1) for precursor concentrations of 0.2, 1.0, and 5.0 wt%, respectively. It should be noted that the peak diameters of the particle size distributions shown in Fig. 11 remained unchanged when the number basis was replaced by a volume basis even though large particles weighed more than small particles on a volume basis. This validated the use of peak drop diameters of 6.8 and 5.5 μm in Fig. 9 for calculation of predicted particle diameters for the 6–9- and 5–8-μm precursor drops whose size distributions were even narrower than those in Fig. 11.

As the precursor drops smaller than 10-μm diameter pass through the reactor, water evaporates at 100°C in less than 3 ms,[14] resulting in particles of ZHA or $Zr(OH)_4$ (due to thermohydrolysis) with diameters much smaller than 3 μm because the precursor molecules are too far apart (see Table I for 5 wt% precursor concentration, 1.5 μm multiplied by 2, the density ratio of zirconia to precursor). The vapor pressure required for 3-μm-diameter particles at 350°C with a characteristic time (the time required to reduce the particle size by half) of 0.1 s is very small (estimated to be 0.4 Torr on the basis of the diffusion model in continuum regime[14]). In addition, due to the Kelvin effect, the vapor pressure over the surface of a small particle is higher than that over the flatter surface of a large particle. In other words, the molecules near the surface of a small particle have fewer nearest neighbors than they would have near a large particle. As a result, less energy is required to remove a molecule from a small particle.[14] Therefore, partial evaporation of ZHA or $Zr(OH)_4$ occurs and conversion to zirconia takes place in the gas phase. In this connection, it should be pointed out that decomposition of ZHA into acetic acid and $Zr(OH)_4$ and subsequent vaporization at temperatures of 175° and 350°C were indeed observed in the aforementioned TGA and DSC analyses. Thus, the gas-to-particle conversion mechanism prevalent in flame combustion spray pyrolysis[11] may be also active in spray pyrolysis at moderate temperatures, as it is the case in this study.

Direct evidence of gas-to-particle conversion is the presence of product particles 20–30-nm diameter, as shown in Fig. 12. These small particles constitute a very significant fraction of particles (35%–40%) obtained in spray pyrolysis of 6–9-μm precursor drops at a maximum reactor temperature of 650°C and 0.01 wt% precursor concentration in a 2.5-cm-diameter reactor. Excluding these 20–30-nm particles, the larger product particles (50–175-nm diameter) had a mean particle diameter of 95 nm. The presence of 20–30-nm particles may be attributed to the short residence time at temperatures of 550°C and above (~0.2 s). In fact, ultrafine particles (<30 nm) have been obtained via gas-to-particle conversion mechanism in spray pyrolysis of precursor metal salts such as metal nitrates.[15]

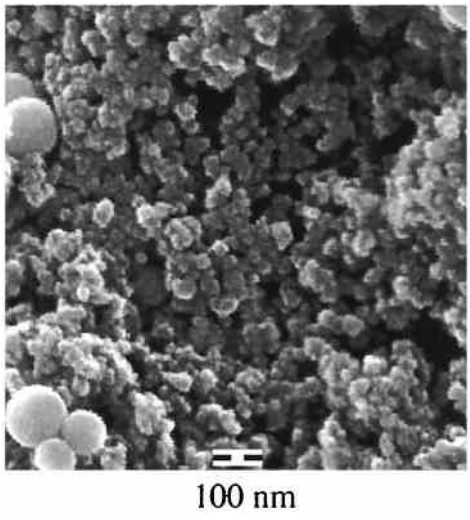

Fig. 12. SEM micrograph of particles from spray pyrolysis at 650°C and carrier airflow rate of 31 L/min using a 2.5-cm-diameter reactor for 0.01 wt% precursor drops of 6–9-μm diameter.

IV. Conclusions

Although the effects of precursor drop size on particle size and morphology in spray pyrolysis have been widely accepted,[1] no studies have critically examined and quantified these effects. This study uses uniform precursor drops generated by an ultrasonic nebulizer and a new atomization technique, ultrasound-modulated two-fluid (UMTF) atomization or air-assisted ultrasonic atomization. The product particle size and uniformity are indeed determined by the precursor drop size and size distribution. Uniform dense spherical nanoparticles of 73-nm diameter were produced by spray pyrolysis through the use of uniform precursor drops (5–8-μm diameter) and a low precursor concentration (0.01 wt%). However, despite much larger precursor drop sizes (peak diameter, 28 μm in UTMF atomization vs 6.8 μm in conventional ultrasonic nebulizer atomization), UMTF spray pyrolysis at 120-kHz ultrasonic frequency and 2.3-W electric drive power generated larger percentages of YSZ particles that were smaller than 0.35-μm diameter (70% with UMTF vs 11% with conventional ultrasonic nebulizer atomization). More importantly, the particles produced in spray pyrolysis of precisely measured precursor drops with a very narrow drop-size distribution were much smaller than those predicted by the one-particle-per-drop mechanism. Presence of 20–30-nm-diameter particles along with larger particles with a mean diameter of 95 nm in spray pyrolysis at 650°C and short residence time (~0.2 s) confirms the activity of gas-to-particle conversion mechanism.

References

[1]G. L. Messing, S.-C. Zhang, and G. V. Jayanthi, "Ceramic Powder Synthesis by Spray Pyrolysis," *J. Am. Ceram. Soc.*, **76** [11] 2707–26 (1993).

[2]Y. C. Kang and S. B. Park, "Preparation of Naometre Size Oxide Particles Using Filter Expansion Aerosol Generator," *J. Mater. Sci.*, **31**, 2409–16 (1996).

[3]O. B. Milosevic, M. J. Mirkovic, and D. P. Uskokovic, "Mechanism of $BaTiO_3$ Powders Prepared by Twin-Fluid and Ultrasonic Spray-Pyrolysis Methods," *J. Am. Ceram. Soc.*, **79** [6] 1720–22 (1996).

[4]S.-C. Zhang and G. L. Messing, "Synthesis of Solid, Spherical Zirconia Particles by Spray Pyrolysis," *J. Am. Ceram. Soc.*, **73** [1] 61–67 (1990).

[5]H. Ishizawa, O. Sakurai, N. Mizutani, and M. Kato, "Homogeneous Y_2O_3-Stabilized ZrO_2 Powder by Spray Pyrolysis Method," *Am. Ceram. Soc. Bull.*, **65** [10] 1399–404 (1986).

[6]S. C. Tsai, P. Childs, and P. Luu, "Ultrasound-Modulated Two-Fluid Atomization of a Water Jet," *AIChE J.*, **42**, 3340–50 (1996).

[7]S. C. Tsai, P. Luu, P. Childs, A. Teshome, and C. S. Tsai, "The Role of Capillary Waves in Two-Fluid Atomization," *Phys. Fluids*, **9**, 2909–18 (1997).

[8]S. C. Tsai, P. Luu, P. Tam, G. Roski, and C. S. Tsai, "Flow Visualization of Taylor-Mode Breakup of a Viscous Jet," *AIP Phys. Fluids*, **11**, 1331–41 (1999).

[9]E. D. Hirleman, V. Oechsle, and N. A. Chigier, "Response Characteristics of Laser Diffraction Particle Size Ananlyzers: Optical Sample Volume Extent and Lens Effects," *Opt. Eng.*, **23**, 610–19 (1984).

[10]R. P. Ingel and D. Lewis III, "Lattice Parameters and Density for Y_2O_3-Stablilized ZrO_2," *J. Am. Ceram. Soc.*, **69** [4] 325–32 (1986).

[11]J. J. Helble, "Combustion Aerosol Synthesis of Nanoscale Ceramic Powders," *J. Aerosol Sci.*, **29**, 721–36 1998.

[12]R. Lang, "Ultrasonic Atomization of Liquids," *J. Acoust. Soc. Am.*, **34**, 7–10 (1962).

[13]Y. Matsuzaki, M. Hishinuma, and I. Yasuda, "Growth of Yttria Stabilized Zirconia Thin Films by Metallo-Organic Ultrasonic Spray Pyrolysis," *Thin Solid Films*, **340**, 72–76 (1999).

[14]T. T. Kodas and M. J. Hampden-Smith, *Aerosol Processing of Materials*; Chs. 4, 8, and 11. Wiley-VCH, New York, 1999.

[15]A. S. Gurav and T. T. Kodas, "Gas-Phase Particle Size Distributions and Lead Loss During Spray Pyrolysis of (Bi, PB)-Sr-Ca-Cu-O," *J. Mater. Res.*, **10**, 1644–52 (1995). □